Dynamical Arrest of Ultracold Lattice Fermions

Schmidt, B.; Reza Bakhtiari, M.; Titvinidze, I.; Schneider, U.; Snoek, M.; Hofstetter, W.

DOI
10.1103/PhysRevLett.110.075302
Publication date
2013
Document Version
Final published version
Published in
Physical Review Letters

Dynamical Arrest of Ultracold Lattice Fermions

Bernd Schmidt,[1] M. Reza Bakhtiari,[1,2] Irakli Titvinidze,[1,2] Ulrich Schneider,[3] Michiel Snoek,[4] and Walter Hofstetter[1]

[1]*Institut für Theoretische Physik, Goethe-Universität Frankfurt, 60438 Frankfurt/Main, Germany*
[2]*I. Institut für Theoretische Physik, Universität Hamburg, 20355 Hamburg, Germany*
[3]*Fakultät für Physik, Ludwig-Maximilians-Universität, 80799 München, Germany*
[4]*Institute for Theoretical Physics, Universiteit van Amsterdam, 1090 GL Amsterdam, The Netherlands*
(Received 13 June 2012; revised manuscript received 5 November 2012; published 12 February 2013)

We theoretically investigate the thermodynamics of an interacting inhomogeneous two-component Fermi gas in an optical lattice. Motivated by a recent experiment by L. Hackermüller *et al.*, Science **327**, 1621 (2010), we study the effect of the interplay between thermodynamics and strong correlations on the size of the fermionic cloud. We use dynamical mean-field theory to compute the cloud size, which in the experiment shows an anomalous expansion behavior upon increasing attractive interaction. We confirm this qualitative effect but, assuming adiabaticity, we find quantitative agreement only for weak interactions. For strong interactions we observe significant nonequilibrium effects which we attribute to a dynamical arrest of the particles due to increasing correlations.

DOI: 10.1103/PhysRevLett.110.075302 PACS numbers: 67.85.−d, 03.75.Ss, 05.30.Fk, 71.10.Fd

Introduction.—At the heart of many condensed-matter phenomena lies the interplay between strong correlations and temperature. However, even the minimal model incorporating these effects, the Hubbard model, withstands an exact solution. Ultracold quantum gases in optical lattices provide a new way to emulate the physics of these model systems in a highly controlled way [1]: not only can almost all system parameters be tuned with ultimate precision, but also the microscopic details underlying the model are fully known. In this way the phase diagram of the Bose-Hubbard model, which includes the bosonic Mott insulator, has been mapped out [2]. For fermionic lattice systems, which directly correspond to electrons in crystalline solid-state lattices, the formation of an incompressible Mott insulating state has been observed as well [3,4]. Using Feshbach resonances, it has also been possible to implement the attractive Hubbard model [5,6], which sustains an s-wave superfluid state at low temperature and entropy.

One ultimate goal of this research direction is to establish a detailed description of the Fermi-Hubbard model applicable to the strongly correlated regime of high-T_c superconductors [7,8]. Unfortunately, current experimental entropies are too high to observe phenomena such as magnetic ordering [9]. While average entropies per particle down to $S/k_BN \sim 0.5$ have been demonstrated for fermions in pure dipole traps [10], in optical lattices only values down to $S/k_BN \sim 1$–2 could be realized so far [6,11], which is well above the maximum entropy where antiferromagnetic ordering can be observed [12,13].

However, even at the current experimental entropies, interesting physics emerges from the interplay between strong correlations and thermodynamics, as has been studied by several authors for repulsive interactions [13–16] in the context of Mott insulators. Recently, Hackermüller *et al.* experimentally [6] investigated this interplay between strong correlations and entropy, focusing on the attractive regime. By loading a two-component Fermi gas into a three-dimensional (3D) optical lattice in the presence of a harmonic trapping potential, the size of the fermionic cloud was measured for different interaction strengths. One would naturally expect that this leads to an increasing cloud size for repulsive interactions while an increasing attractive interaction should lead to a decreasing cloud size. However, a counterintuitive behavior of the cloud size was observed: the cloud shrinks upon entering the attractive regime, but reaches a minimum at relatively small attractive interaction. For larger attraction the cloud expands again.

This anomalous trend was attributed to the adiabatic heating effect: for sufficiently strong attractive interaction, singly occupied sites have a much higher energy than doubly occupied ones and become energetically irrelevant. This strongly reduces the available Hilbert space and, at constant temperature, leads to a lower entropy. In order to keep the entropy constant, the temperature increases, leading to a higher entropy in the motional degree of freedom and therefore to the anomalous expansion.

In this Letter we theoretically investigate this experiment by means of dynamical mean-field theory (DMFT) simulations of the Hubbard model in the presence of a harmonic trap. Even though our calculations fully include the adiabatic heating effect and also find an anomalous expansion of the cloud size for large attractive interactions, we only find an agreement between our equilibrium calculation and the experimental data of Ref. [6] for weak interactions, whereas we find a significant discrepancy for strong interactions. We attribute this to a strong slowing down of particle transport already for moderately large interactions, leading to a *dynamical arrest* in a state whose size is significantly larger than the equilibrium radius of the

particle cloud. The long-lived arrested states, which we find for lattice fermions, bear a strong resemblance to those of attractive colloidal glasses [17].

Model and method.—We consider a two-component mixture of fermionic atoms, loaded into the lowest band of a 3D cubic optical lattice in the presence of an external harmonic potential. For sufficiently deep optical lattices, this system is well described by the inhomogeneous Fermi-Hubbard Hamiltonian

$$\mathcal{H} = -J \sum_{\langle i,j\rangle,\sigma} (\hat{c}^{\dagger}_{i\sigma}\hat{c}_{j\sigma} + \text{H.c.}) + U\sum_i \hat{n}_{i\uparrow}\hat{n}_{i\downarrow} - \sum_{i\sigma}(\mu - V_0 r_i^2)\hat{n}_{i\sigma}.$$

Here, $\hat{c}^{\dagger}_{i\sigma}$ and $\hat{c}_{i\sigma}$ are the fermionic creation and annihilation operators and $\hat{n}_{i\sigma} = \hat{c}^{\dagger}_{i\sigma}\hat{c}_{i\sigma}$ is the number operator, where $\sigma \in \{\uparrow, \downarrow\}$ labels the two hyperfine states. The on-site interaction is denoted by U, the single-atom hopping amplitude between nearest neighbors $\langle i, j\rangle$ is J and μ is the chemical potential controlling the particle number. We consider a pancake shaped harmonic trapping potential of strength V_0 with aspect ratio γ and define $r_i^2 = x_i^2 + y_i^2 + \gamma^2 z_i^2$ as the squared distance of site i from the trap center.

We apply DMFT to obtain the *equilibrium* properties of this Hamiltonian. Employing the assumption of a local self-energy, DMFT treats local quantum correlations in a fully nonperturbative manner [18]. The Fermi-Hubbard model is mapped to an effective single impurity Anderson model. Here we use exact diagonalization to obtain the self-consistent solution of the impurity model with 3 auxiliary bath degrees of freedom in the effective single impurity Anderson model, to obtain the self-consistent solution. We determine the local Green's function for the lowest 200 Matsubara frequencies. To incorporate the harmonic potential, we use the local density approximation (LDA), which is known to reliably predict the density distribution for fermionic systems when the trap is sufficiently shallow [19,20]. In this approximation, every site is modeled as part of a homogeneous system with local chemical potential $\mu(r_i) = \mu_0 - V_0 r_i^2$. We obtain the density profile of the fermions, from which the cloud radius is extracted. To make a direct comparison with the experiment, we employ the following definition for the cloud radius [6]

$$R^2 = \frac{1}{N_\sigma}\sum_i r_i^2 \langle \hat{n}_{i,\sigma}\rangle, \tag{1}$$

where N_σ is the total particle number per spin state. We consider a balanced mixture with total particle number $N = 2N_\sigma$, such that R in Eq. (1) is independent of σ. To compute the entropy per lattice site, we use the Maxwell relation $s(\mu) = \int_{-\infty}^{\mu} d\mu' \partial n(\mu')/\partial T$ and then obtain the total entropy by $S = \sum_i s[\mu(r_i)]$. The harmonic potential is characterized by the characteristic energy $E_c = V_0 r_c^2 = \frac{3}{5} V_0 (3\gamma N/8\pi)^{2/3}$, which is the mean potential energy per particle of a maximally packed state at the bottom of the trap with total particle number N; r_c is the corresponding radius, which is used as the length scale to express the cloud size R/r_c. We note that in LDA the rescaled radius R/r_c is fully determined by the average entropy per particle $S/k_B N$ and the ratios of tunneling to trap strength J/E_c and interaction to tunneling U/J, implying that all results shown in Figs. 1–5 are independent of the details of the trap. The experiment has been performed for $N_\sigma \approx 1.5 \times 10^5$ particles at a temperature $T/T_F = 0.12 \pm 0.03$ before loading of the lattice (where T_F is the Fermi temperature) and an entropy per particle of $S/k_B N = 1.15 \pm 0.25$. In the experiment, both $S/k_B N$ and J/E_c were known only with a considerable uncertainty [6]. Since the effect of the experimental uncertainty in J/E_c on the cloud size is larger, we chose to perform all calculations for a fixed entropy per particle of $S/k_B N = 1.15$ and determined the value of J/E_c by comparing the experimental radius for $U/J = 0$ with exact diagonalization (ED) results. In the noninteracting case nonequilibrium effects are minimal, so that the experimental data at $U/J = 0$ can be reliably fitted to theoretical calculations [21]. The resulting J/E_c agree with the experimental data within error bars for low confinements, and only deviate at high confinements, where also some heating was observed in the experiment (cf. Supplemental Material to Ref. [6]). In addition, we find satisfying quantitative agreement with our DMFT

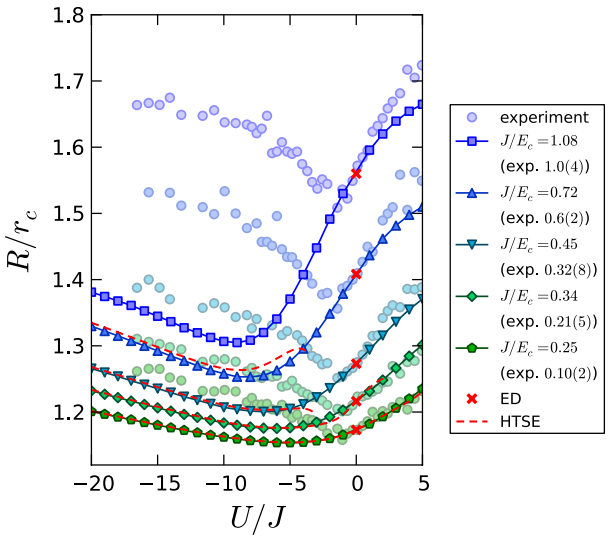

FIG. 1 (color online). Comparison of the experimental cloud radius with DMFT results [23]. While we find good agreement for small interactions, the experimentally observed radii are significantly higher than expected from theory for stronger interactions. We attribute this to the dynamical arrest discussed in the main text. Also shown are the results of a 6th order high temperature series expansion (HTSE) of the Hubbard model (dashed lines) [24,25]. Since temperature decreases with increasing J/E_c and U/J [cf. Fig. 2 (left)] the HTSE is only applicable to sufficiently small or negative U/J and small J/E_c.

calculations for the fixed J/E_c (without additional fitting parameters) in the regime of weak interactions.

Results.—In Fig. 1 we show our DMFT results for the rescaled cloud radius R/r_c versus the on-site interaction U/J for various values of the characteristic trap energy J/E_c, which are compared directly to the experimental data points [6]. Also, a comparison with a 6th order high temperature series expansion is included in this figure, which agrees very well with the DMFT calculations. While we included the possibility of s-wave superfluid order in our calculations, we found that the experimental entropy is too high for superfluidity to be present.

For weak interactions $|U/J| \lesssim 2$, we observe very good quantitative agreement with the experimental data points, evidencing that the DMFT solution of the single-band Hubbard model incorporates the relevant physics in this parameter regime. For stronger attractive interactions we also find the anomalous expansion of the cloud size in the DMFT calculations. By plotting the temperature at constant entropy, we can directly verify that this is indeed due to adiabatic heating originating from a reduced available phase space. This is displayed in Fig. 2 (left) and indeed shows a strong rise for large attraction. When the entropy is decreased, the anomalous expansion is expected to disappear, since essentially ground state properties are probed in this case. This is clearly visible in Fig. 2 (right), where the radius for different entropies is shown. For repulsive interactions an adiabatic cooling effect is observed, similar to what was found in Ref. [12] (see Supplemental Material of Ref. [4]). Although for strong repulsion a similar reduction in phase space occurs, because doubly occupied sites are energetically unfavored, this is more than compensated by additional (spin) configurational entropy for the fermions at the wings of the clouds.

Although our simulation thus fully includes the adiabatic heating effect, our results show that the anomalous expansion seen in the experiment cannot be explained by adiabatic heating alone: At stronger interactions we find significant deviations from the experimentally observed cloud sizes, which are much larger than theoretically expected. By measuring the temperature after unloading the atoms again from the lattice it was excluded that the discrepancy is due to heating [6]. We attribute this difference to strong nonequilibrium effects in the loading: after evaporative cooling, the cloud size in the pure harmonic trap is significantly larger than the final equilibrium size in the lattice. During the ramp-up of the lattice, the effective mass of the atoms increases due to a reduction of kinetic energy in the lowest band of the lattice. This leads to a shrinking of the cloud (see Fig. 3) under adiabatic conditions. The scattering length, which is adjusted by using a Feshbach resonance before the loading of the lattice, gives rise to an interaction strength U/J which rapidly grows with the lattice depth. As recently demonstrated [21], even moderate interactions slow down the atoms severely, thereby prohibiting the large-scale particle transport necessary for following the adiabatic path. This can be seen, e.g., by comparing the initial radius before the ramp-up with the radius in the lattice [Fig. 4 (left)]: In the experiment, the radius shrinks always by the same percentage independently of the trap strength, which would not be the case if the cloud stays in equilibrium. In contrast to the situation in Ref. [21], where a symmetric reduction of particle transport for attractive and repulsive interactions was observed, we observe much weaker non-adiabatic effects for the repulsive regime in this case. This is probably due to the fact that the difference between the radius before the ramp-up and the equilibrium radius at the final lattice depth is much smaller in the repulsive than in the attractive regime. Once this effect is scaled out [see Fig. 4 (right)] we see a significant deviation on both sides. Moreover, repulsive interactions decrease the number of double occupancies while attractive interactions increase it, thereby giving rise to different dynamics. Interestingly, we see that the deviation in Fig. 4 (right) becomes

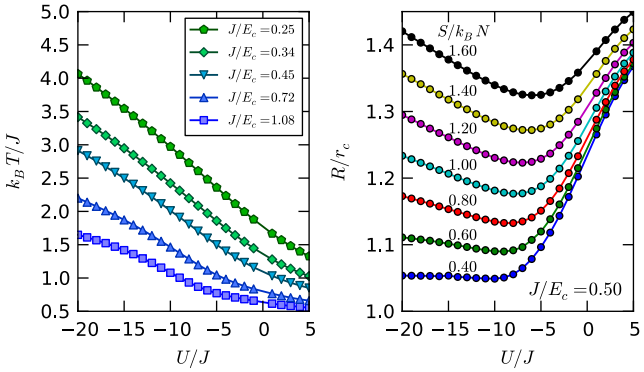

FIG. 2 (color online). Left: Temperature vs interaction for an entropy per particle of $S/k_B N = 1.15$ and different external harmonic confinements. Right: Cloud radius for different entropies $S/k_B N = 0.4$–1.6. The anomalous expansion becomes more pronounced for higher entropies.

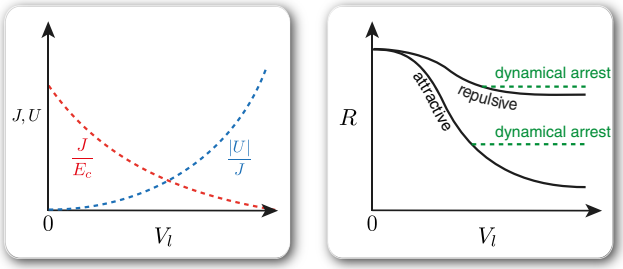

FIG. 3 (color online). Interacting fermions during the lattice ramp up: In the experiment, the harmonic confinement E_c and the scattering length are set in the dipole trap and remain fixed during the lattice ramp. Left: The tunneling and interaction during the ramp. Right: Equilibrium cloud size for attractive and repulsive interactions during the ramp. The dashed line denotes the nonadiabatic path of the dynamical arrest.

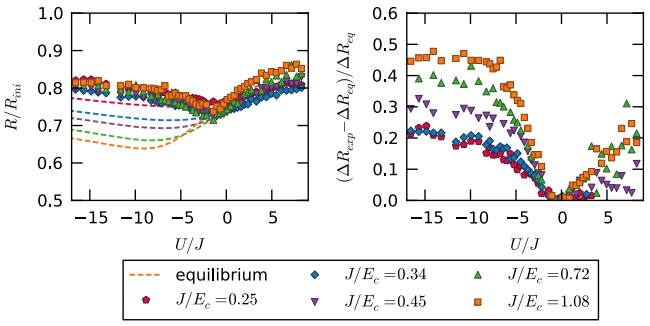

FIG. 4 (color online). Left: Final radius R of the cloud relative to the initial radius R_{ini} before ramp-up of the lattice. (symbols: experiment, lines: equilibrium theory, same colors denote same J/E_c) Right: Relative difference between expected ($\Delta R_{\mathrm{eq}} = R_{\mathrm{eq}} - R_{\mathrm{ini}}$) and observed ($\Delta R_{\mathrm{exp}} = R_{\mathrm{exp}} - R_{\mathrm{ini}}$) change in cloud size during the lattice loading from the expected change in cloud size during the ramp.

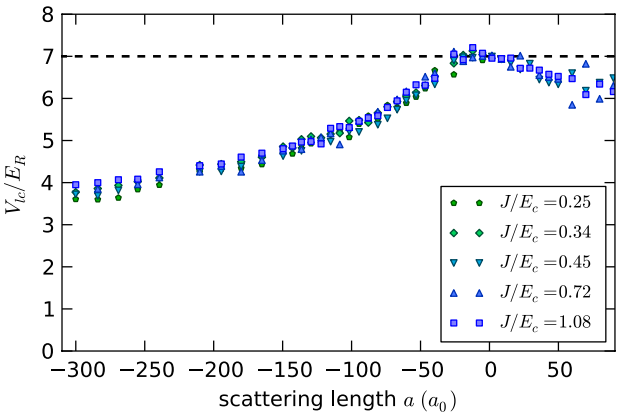

FIG. 5 (color online). Critical lattice depth calculated from the experimentally measured radius via Eq. (2), as a function of the scattering length. The dashed line indicates the final maximum lattice depth at $V_l/E_R = 7$ to which the optical lattice was ramped up. The values for J/E_c given in the legend are reached for lattice depth $7E_R$.

independent of U/J for sufficiently strong attraction. This is because the experimental and theoretical curves in Fig. 1—although offset—have the same slope.

To quantify the proposed scenario, i.e., that the disagreement between the experimental and theoretical cloud size has to be attributed to a dynamical arrest of the particles due to the slowing down of particle transport, we substitute this gradual change in adiabaticity by a stepwise model where up to a critical lattice depth V_{lc} the system is in thermal and chemical equilibrium and experiences fully adiabatic changes of its state. When the lattice depth exceeds a critical value we assume the cloud to be completely static, as illustrated in Fig. 3.

Within this model we only need equilibrium simulations to determine the critical lattice depth. As seen before, within LDA the rescaled radius $\tilde{R} = R/r_c$ depends only on $\tilde{S} = S/k_B N$, $\tilde{J} = J/E_c$ and $\tilde{U} = U/J$. This allows us to determine the lattice depth at which the system freezes by calculating $\tilde{J} = \tilde{J}(\tilde{V}_l)$ and $\tilde{U} = \tilde{U}(\tilde{V}_l, \tilde{a})$ as a function of the lattice depth $\tilde{V}_l = V_l/E_R$ using band structure calculations. Here, $\tilde{a} = a/a_0$ (a_0: Bohr radius) denotes the scattering length. We take into account that E_c also depends on the lattice depth due to the anticonfining effect of the optical lattice. The critical lattice depth V_{lc} is then defined as the value, where the calculated equilibrium radius coincides with the experimentally measured one; i.e.,

$$\tilde{R}_{\mathrm{exp}} = \tilde{R}(\tilde{S}, \tilde{J}(\tilde{V}_{lc}), \tilde{U}(\tilde{V}_{lc}, \tilde{a})), \tag{2}$$

where $\tilde{R}_{\mathrm{exp}}$ is the experimentally measured radius and the function $\tilde{R}$ is calculated with DMFT.

The resulting critical lattice depths V_{lc} for dynamical arrest of the cloud are shown in Fig. 5. First, we observe a strong dependence on the scattering length, which is indeed fully consistent with the dynamical arrest hypothesis, as the scattering length linearly affects U/J, which determines the transport properties. We note that for stronger interactions the critical lattice depth is rather low, and almost leaves the validity regime of the single-band Hubbard model. Second, we observe that V_{lc} is relatively independent of the external harmonic confinement V_0, such that the data points for different J/E_c collapse almost to a single curve. Indeed, while a tighter trap increases the density and thereby slows down the dynamics, it at the same time also decreases the distance for the required particle transport.

Conclusion.—We calculated the cloud size of an interacting Fermi gas by means of DMFT and obtained very good quantitative agreement with experimental data for weak interactions. Despite qualitative agreement, we observe a significant discrepancy with the experiment for strong interactions, which we attribute to nonequilibrium effects caused by an interaction-induced slowing down of particle transport. The system is therefore dynamically arrested at a critical lattice depth, which we observe to be almost independent of the harmonic trap. The observation of such an arrested state gives very interesting insights into the nonequilibrium dynamics of strongly interacting many-particle systems: it shows that the velocity for mass transport and (probably) entropy transport decreases very fast with increasing interaction, such that strongly interacting systems are nearly frozen. This message clearly has far-reaching consequences for future experiments on strongly interacting Fermi gases in optical lattices, for instance, with the goal of observing s-wave superfluidity or antiferromagnetic order. The dynamical arrest makes it difficult to prepare the system in the desired equilibrium states. Avoiding the dynamical arrest requires broad changes of the experimental procedures used up to now: any loading sequence into a deep lattice should be tailored such that it minimizes the required density and entropy redistribution. Concerning

particle transport, this could in principle be achieved by dynamically adjusting the trapping potential during the lattice loading. However, the formation of the desired low-entropy phases in addition requires a strong redistribution of entropy, which will probably be subject to similar limitations. In the case of the antiferromagnet, another possibility is the recently proposed use of a superlattice [22]: There, the atoms would initially be loaded into a noninteracting band insulator in the long wavelength lattice, thus avoiding the dynamical arrest of interacting particles. Subsequently, this state can be adiabatically transformed into an antiferromagnet in the short wavelength lattice without any density or entropy redistributions.

We would like to acknowledge useful discussions with I. Bloch. This work was supported by the German Science Foundation DFG (FOR 801, SFB/TR 49, SFB 668, and SFB 925) and the Netherlands Organization for Scientific Research (NWO).

[1] I. Bloch, J. Dalibard, and W. Zwerger, Rev. Mod. Phys. **80**, 885 (2008).
[2] M. Greiner, O. Mandel, T. Esslinger, T. Hansch, and I. Bloch, Nature (London) **415**, 39 (2002).
[3] R. Jördens, N. Strohmaier, K. Günther, H. Moritz, and T. Esslinger, Nature (London) **455**, 204 (2008).
[4] U. Schneider, L. Hackermüller, S. Will, T. Best, I. Bloch, T. A. Costi, R. W. Helmes, D. Rasch, and A. Rosch, Science **322**, 1520 (2008).
[5] N. Strohmaier, Y. Takasu, K. Günter, R. Jördens, M. Köhl, H. Moritz, and T. Esslinger, Phys. Rev. Lett. **99**, 220601 (2007).
[6] L. Hackermüller, U. Schneider, M. Moreno-Cardoner, T. Kitagawa, T. Best, S. Will, E. Demler, E. Altman, I. Bloch, and B. Paredes, Science **327**, 1621 (2010).
[7] T. Esslinger, Annu. Rev. Condens. Matter Phys. **1**, 129 (2010).
[8] W. Hofstetter, J. I. Cirac, P. Zoller, E. Demler, and M. D. Lukin, Phys. Rev. Lett. **89**, 220407 (2002).
[9] D. McKay and B. DeMarco, Rep. Prog. Phys. **74**, 054401 (2011).
[10] T.-L. Ho and Q. Zhou, Proc. Natl. Acad. Sci. U.S.A. **106**, 6916 (2009).
[11] D. Greif, L. Tarruell, T. Uehlinger, R. Jördens, and T. Esslinger, Phys. Rev. Lett. **106**, 145302 (2011).
[12] T. Paiva, Y. L. Loh, M. Randeria, R. T. Scalettar, and N. Trivedi, Phys. Rev. Lett. **107**, 086401 (2011).
[13] S. Fuchs, E. Gull, L. Pollet, E. Burovski, E. Kozik, T. Pruschke, and M. Troyer, Phys. Rev. Lett. **106**, 030401 (2011).
[14] L. De Leo, C. Kollath, A. Georges, M. Ferrero, and O. Parcollet, Phys. Rev. Lett. **101**, 210403 (2008).
[15] R. Jördens, L. Tarruell, D. Greif, T. Uehlinger, N. Strohmaier, H. Moritz, T. Esslinger, L. De Leo, C. Kollath, A. Georges, V. Scarola, L. Pollet, E. Burovski, E. Kozik, and M. Troyer, Phys. Rev. Lett. **104**, 180401 (2010).
[16] E. Khatami and M. Rigol, Phys. Rev. A **84**, 053611 (2011).
[17] K. A. Dawson, Curr. Opin. Colloid Interface Sci. **7**, 218 (2002).
[18] A. Georges, G. Kotliar, W. Krauth, and M. J. Rozenberg, Rev. Mod. Phys. **68**, 13 (1996).
[19] R. W. Helmes, T. A. Costi, and A. Rosch, Phys. Rev. Lett. **100**, 056403 (2008).
[20] M. Snoek, I. Titvinidze, C. Toke, K. Byczuk, and W. Hofstetter, New J. Phys. **10**, 093008 (2008).
[21] U. Schneider, L. Hackermüller, J. P. Ronzheimer, S. Will, S. Braun, T. Best, I. Bloch, E. Demler, S. Mandt, D. Rasch, and A. Rosch, Nat. Phys. **8**, 213 (2012).
[22] M. Lubasch, V. Murg, U. Schneider, J. I. Cirac, and M.-C. Bañuls, Phys. Rev. Lett. **107**, 165301 (2011).
[23] Compared to the plots in Ref. [6], the experimental data include an updated parametrization of the Feshbach resonance.
[24] J. A. Henderson, J. Oitmaa, and M. C. B. Ashley, Phys. Rev. B **46**, 6328 (1992).
[25] D. F. B. ten Haaf and J. M. J. van Leeuwen, Phys. Rev. B **46**, 6313 (1992).